Simulation of Surface Plasmon Resonance (SPR) in the Kretschmann Configuration (FEniCS & COMSOL)

Alireza Alinejad[a]

[a]*Prof. Jost Adam, CMP-dep., University of Kassel*

Abstract

Surface plasmon resonance (SPR) in the Kretschmann configuration provides a compact, sensitive platform for refractive-index sensing. We consider a multilayer stack comprising a glass prism, a gold film, a graphene monolayer, and an aqueous sensing medium. For a TM-polarized He–Ne laser ($\lambda = 633\,\mathrm{nm}$), we derive the governing equations from Maxwell's theory, state boundary and interface conditions, formulate the weak (variational) form suitable for finite-element discretization, and outline reproducible modeling steps in both FEniCS and COMSOL. Analytical transfer-matrix calculations are used as a reference to validate the finite-element results.

Keywords: Surface plasmon resonance, Kretschmann configuration, Graphene, Finite element method, FEniCS, COMSOL, PML

1. Introduction

Plasmonics explores the coupling of light with collective electron oscillations at metal interfaces. Among its hallmark phenomena is surface plasmon resonance (SPR), which enables strong field confinement and extraordinary sensitivity to refractive-index changes near a metal surface. Since the seminal prism-coupling experiments of Kretschmann and Raether [1], SPR has become a workhorse of label-free chemical and biosensing.

This study targets the CMP mini-project [2]: to model SPR in a prism/metal/2D monolayer/water stack using FEM, locate the resonance angle for $\lambda = 633\,\mathrm{nm}$, and analyze parametric effects (metal choice, 2D layer, thickness) with a focus on a gold film plus a graphene monolayer. We implement the problem in FEniCS (open-source FEM) and COMSOL (commercial FEM) for cross-validation.

2. Theory and Physics Background

2.1. Maxwell Equations and Helmholtz Form

For time-harmonic fields $e^{-i\omega t}$, Maxwell's equations reduce to the vector Helmholtz form [3]

$$\nabla \times \left(\mu_r^{-1} \nabla \times \mathbf{E}\right) - k_0^2 \varepsilon_r \mathbf{E} = \mathbf{0}, \qquad k_0 = \frac{2\pi}{\lambda}. \tag{1}$$

2.2. SPP Dispersion and Kretschmann Coupling

For a planar metal–dielectric interface, the SPP dispersion is [4]

$$\beta(\omega) = \frac{\omega}{c}\sqrt{\frac{\varepsilon_m \varepsilon_d}{\varepsilon_m + \varepsilon_d}}. \tag{2}$$

In Kretschmann coupling, a high-index prism provides momentum matching:

$$n_p k_0 \sin\theta = \mathrm{Re}\{\beta\}. \tag{3}$$

2.3. Material Models

Gold's optical constants use Johnson–Christy data [5]. Graphene is included as a monolayer of effective thickness $t = 0.34\,\mathrm{nm}$, which significantly modifies the resonance [6].

2.4. Graphene Modeling via Surface Conductivity

Graphene's optical response is rigorously described by a frequency-dependent *surface conductivity* $\sigma(\omega)$ (Kubo formula; intraband + interband) [6]:

$$\sigma(\omega) = \sigma_{\mathrm{intra}}(\omega) + \sigma_{\mathrm{inter}}(\omega), \tag{4}$$

and for undoped graphene in the visible, the *universal conductivity* $\sigma_0 = \frac{e^2}{4\hbar} \approx 6.08 \times 10^{-5}\,\mathrm{S}$ is a good approximation.

At an interface Γ containing graphene, Maxwell boundary conditions read

$$\mathbf{n} \times (\mathbf{E}_2 - \mathbf{E}_1) = \mathbf{0}, \tag{5}$$

$$\mathbf{n} \times (\mathbf{H}_2 - \mathbf{H}_1) = \sigma(\omega)\,\mathbf{E}_t, \tag{6}$$

i.e. tangential $\mathbf{E}$ is continuous while tangential $\mathbf{H}$ has a jump equal to the induced sheet current.

In the transfer-matrix method (TMM), graphene can be inserted as an *interface sheet* with admittance $\sigma(\omega)$. For TM polarization,

$$r_p^{(\sigma)} = \frac{Y_2^{\mathrm{TM}} - Y_1^{\mathrm{TM}} - \sigma}{Y_2^{\mathrm{TM}} + Y_1^{\mathrm{TM}} + \sigma}, \qquad t_p^{(\sigma)} = \frac{2Y_2^{\mathrm{TM}}}{Y_2^{\mathrm{TM}} + Y_1^{\mathrm{TM}} + \sigma}, \tag{7}$$

where $Y_i^{\mathrm{TM}} = \varepsilon_i \omega / k_{z,i}$. Equivalently, a 2×2 sheet matrix $\mathbf{M}_{\mathrm{sheet}} = \begin{bmatrix} 1 & 0 \\ \sigma & 1 \end{bmatrix}$.

In finite elements, graphene appears as a surface term in the weak form:

$$-i\omega\mu_0 \int_\Gamma \sigma(\omega)\,\mathbf{v}_t^* \cdot \mathbf{E}_t\, dS, \tag{8}$$

a Robin-type contribution that is straightforward in FEniCS/COMSOL.

Thin-film equivalence.. A common shortcut is an ultra-thin film of thickness $d_{\mathrm{eff}} \approx 0.34\,\mathrm{nm}$ with n_{eff}. The mapping is

$$\sigma(\omega) = -\,i\,\varepsilon_0 \omega d_{\mathrm{eff}}\,[\varepsilon_{\mathrm{eff}}(\omega) - 1], \qquad \varepsilon_{\mathrm{eff}} = n_{\mathrm{eff}}^2. \tag{9}$$

With $n_{\mathrm{eff}} \approx 3.0 - 1.4i$ at $\lambda = 633\,\mathrm{nm}$, the implied conductivity is close to σ_0, explaining why the thin-film trick reproduces realistic resonance shifts while the sheet model remains fundamental.

3. Mathematical (FEM) Formulation

3.1. Weak Form and Discretization

Starting from the strong form above, multiply by a test function and integrate by parts to obtain the standard curl–curl weak form. We use complex ε_r, add PMLs, and (for TM) solve a scalar H_z formulation. Nédélec (edge) elements are preferred for full-vector accuracy; in the scalar TM reduction, Lagrange elements suffice. Mesh is refined across Au and graphene to resolve skin depth and evanescent decay.

3.2. Boundary and Interface Conditions

The prism boundary is driven by a TM plane-wave/port at angle θ; the opposite side is absorbing; lateral sides/PMLs prevent spurious reflections [7]. Tangential $\mathbf{E}$ and $\mathbf{H}$ are continuous at interfaces; graphene contributes the sheet term above.

4. Project Description and Geometry

Following the CMP brief [2]:

- Prism (glass): $n_p = 1.50$, thickness $1\,\mu\text{m}$.
- Gold: $d_{\text{Au}} = 40\,\text{nm}$ to $60\,\text{nm}$.
- Graphene: $d_g = 0.34\,\text{nm}$ (thin-film equivalence).
- Sensing region: water, $n_s = 1.33$, thickness $1\,\mu\text{m}$–$1.5\,\mu\text{m}$.
- Width: $2\,\mu\text{m}$–$3\,\mu\text{m}$.
- Illumination: TM, $\lambda = 633\,\text{nm}$, sweep $\theta \in [0^\circ, 90^\circ]$.
- PML thickness: $\approx 0.3\,\mu\text{m}$.

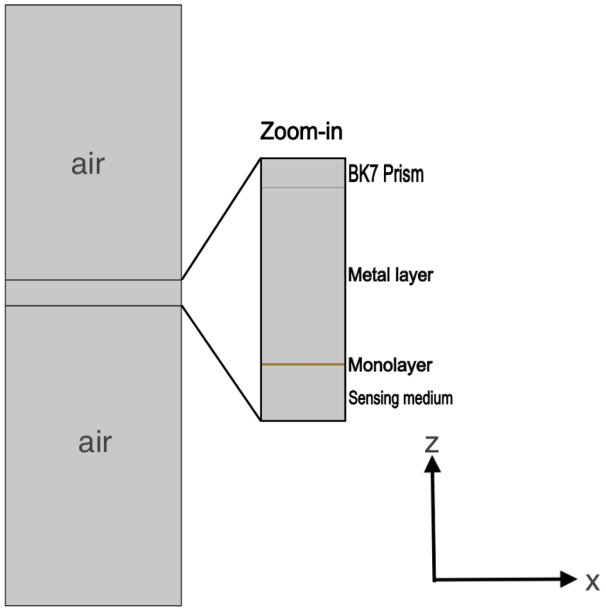

Figure 1: Schematic of the simulated multilayer stack (Prism|Au|Graphene|Water) used in the CMP project. Thicknesses and refractive indices are as given in Sec. 1.

5. Computational Overview

5.1. FEniCS plan

1. Define 2D geometry and subdomains.
2. Assign complex ε_r for graphene layer; implement a custom absorbing boundary trick (surface loss / coordinate stretching) to mimic PML behavior.
3. Assemble weak form; sweep incident angle θ.
4. Compute reflectance-like metric at the prism port; extract θ_{res}.

5.2. COMSOL plan

1. Wave-Optics (Frequency Domain); TM port excitation.
2. Materials: Au (Johnson–Christy), graphene thin film, water(sensing medium).
3. Angle sweep; optional thickness/refractive-index sweeps.
4. Extract reflectance $R(\theta)$ and field maps.

5.3. Performance metrics

- Resonance angle θ_{res}: COMSOL 72.70°; TMM 72.79°.
- Angular FWHM: COMSOL 5.00°; TMM 4.06°.
- Sensitivity $S_\theta = \Delta\theta_{\text{res}}/\Delta n$: TMM $\approx$ **158.75 deg/RIU** near $n_s = 1.33$.
- Angular quality factor $Q_\theta = \theta_{\text{res}}/\text{FWHM}$: COMSOL ≈ 14.53.
- Dip contrast $\mathcal{C} = (R_{\text{baseline}} - R_{\min})/R_{\text{baseline}}$: COMSOL ≈ 0.918.

6. Analytical Model: TM Transfer Matrix (Prism—Au—Graphene—Water)

Let $k_0 = 2\pi/\lambda$, $k_x = k_0 n_0 \sin\theta$, and

$$k_{z,i} = \sqrt{(k_0 n_i)^2 - k_x^2}, \qquad q_i = \frac{k_{z,i}}{k_0 n_i^2}. \tag{10}$$

For a film of thickness d_i,

$$\mathbf{M}_i = \begin{bmatrix} \cos\beta_i & -i\,\dfrac{\sin\beta_i}{q_i} \\ -i\,q_i \sin\beta_i & \cos\beta_i \end{bmatrix}, \quad \beta_i = k_{z,i} d_i. \tag{11}$$

With $\mathbf{M} = \mathbf{M}_1\mathbf{M}_2$ (Au and graphene) and q_0, q_s for prism and sensing medium,

$$r(\theta) = \frac{(M_{11} + M_{12}q_s)q_0 - (M_{21} + M_{22}q_s)}{(M_{11} + M_{12}q_s)q_0 + (M_{21} + M_{22}q_s)}, \qquad R(\theta) = |r(\theta)|^2. \tag{12}$$

Numerical values.. For $\lambda = 633\,\text{nm}$, $n_0 = 1.50$, $d_{\text{Au}} = 50\,\text{nm}$ (Johnson–Christy [5]), graphene thin film $n_g \approx 3.0 - 1.4i$, $d_g = 0.34\,\text{nm}$, and water $n_s = 1.33$, the calculated curve (Fig. 2) yields $\theta_{\text{res}} \approx 72.79^\circ$, $R_{\min} \approx 3.92 \times 10^{-3}$, FWHM $\approx 4.83^\circ$. These serve as targets for the FEM models and help tune mesh/PMLs.

Table 1: Parameters used in the analytical TMM (Prism|Au|Graphene|Water).

Layer / Parameter	**Value**	**Reference**
Prism refractive index n_p	1.50 (BK7 glass)	–
Au refractive index @ 633 nm	$0.19 + 3.59i$	[5]
Au thickness d_{Au}	50 nm	[2]
Graphene refractive index n_g	$3.0 - 1.4i$	[6]
Graphene thickness d_g	0.34 nm	monolayer spacing
Sensing medium (water) n_s	1.33	–
Wavelength λ	633 nm (He–Ne)	[2]

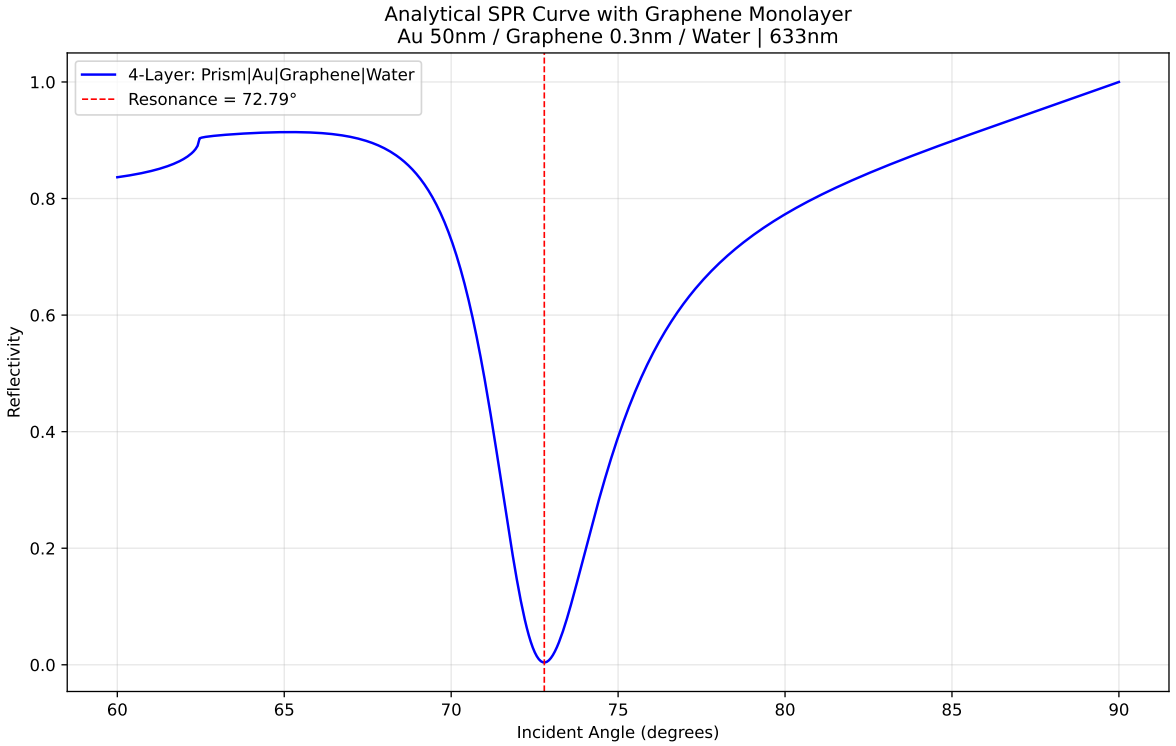

Figure 2: Analytical SPR (TM TMM) for Prism|Au(50 nm)|Graphene(0.34 nm)|Water at $\lambda = 633$ nm. The dashed line marks θ_{res}.

7. Results and Discussion

7.1. FEniCS (quick check)

Figure 3 shows a coarse proof-of-life sweep using a simplified TM setup. The curve is not a strict reflectance (it is a normalized field variation), so the dip does not equal $R_{\min}$, but the angular trend still reveals a resonance-like feature.

FEniCS setup (TM, 2D).. Scalar H_z formulation with complex ε_r; custom absorbing layers at the exit/side boundaries (a "surface trick" instead of a true PML); oblique plane-wave drive at the prism port. Graphene is represented as an ultrathin film (0.34 nm, $n_g \approx 3.0 - 1.4i$), equivalent to a surface-conductivity sheet in the weak form. The mesh is strongly refined across Au/graphene. An angle sweep yields a reflectance-like metric at the port; the dip aligns with the analytical TMM trend.

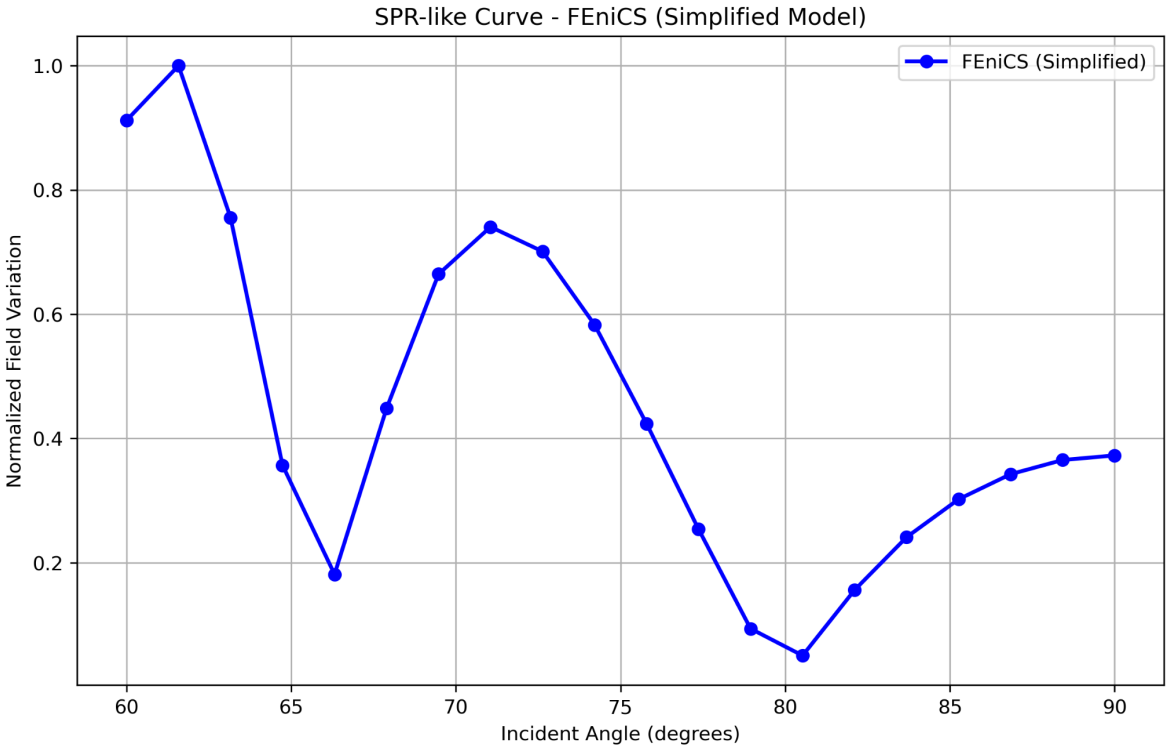

Figure 3: SPR-like curve from the simplified FEniCS model (sanity check).

7.2. FEniCS (final reflectance sweep)

With PMLs, absorbing exit, and TM excitation, the refined FEniCS run yields the normalized reflectance-like curve in Fig. 4. The broad minimum at high θ is consistent with Kretschmann coupling at $\lambda = 633\,\text{nm}$. (Values reflect our material set and mesh grading; they serve as qualitative cross-checks.)

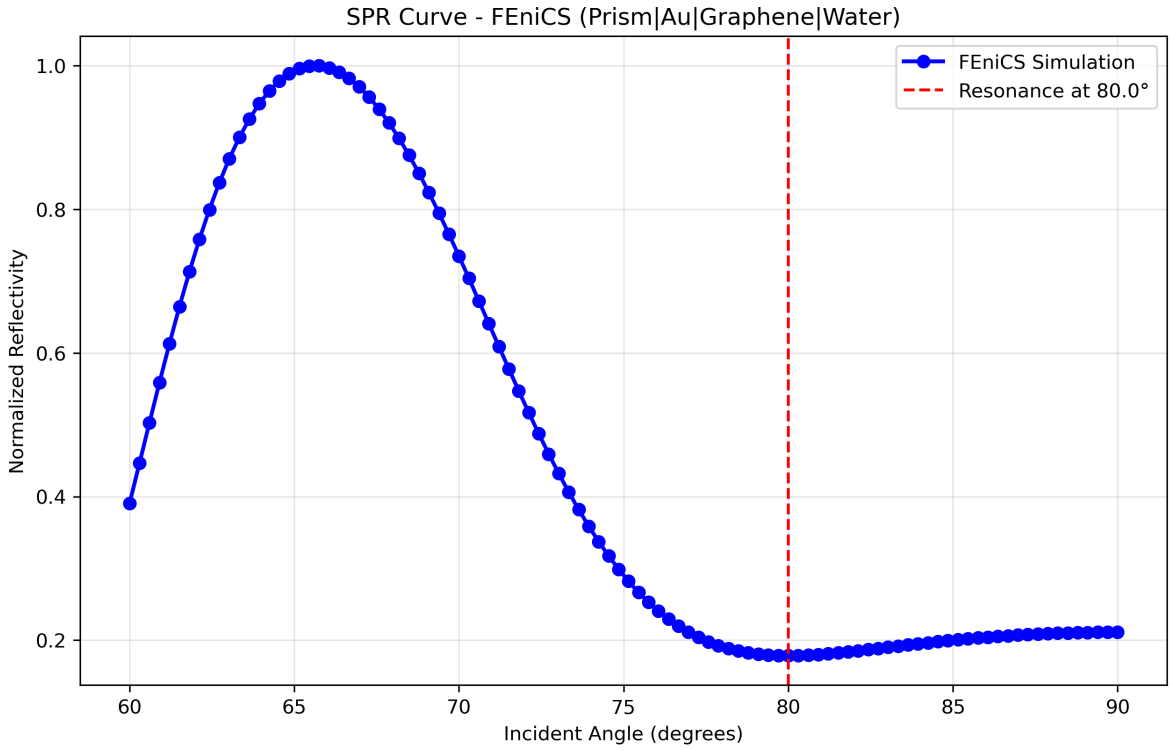

Figure 4: FEniCS sweep (Prism|Au|Graphene|Water). The dip marks the SPR region.

7.3. COMSOL sweep

COMSOL's frequency-domain TM sweep produces the expected sharp dip. From the exported table we obtain $\theta_{\text{res}} = 72.70°$ and $R_{\min} \approx 0.0684$. Using a local-baseline definition, the angular FWHM $\approx 5.00°$, which gives an angular quality factor $Q_\theta = \theta_{\text{res}}/\text{FWHM} \approx 14.53$. The dip contrast relative to the local baseline is $\mathcal{C} \approx 0.918$ (Fig. 5). Small differences vs. FEniCS arise from discretization near Au/graphene, the absorbing-boundary treatment, and port normalization.

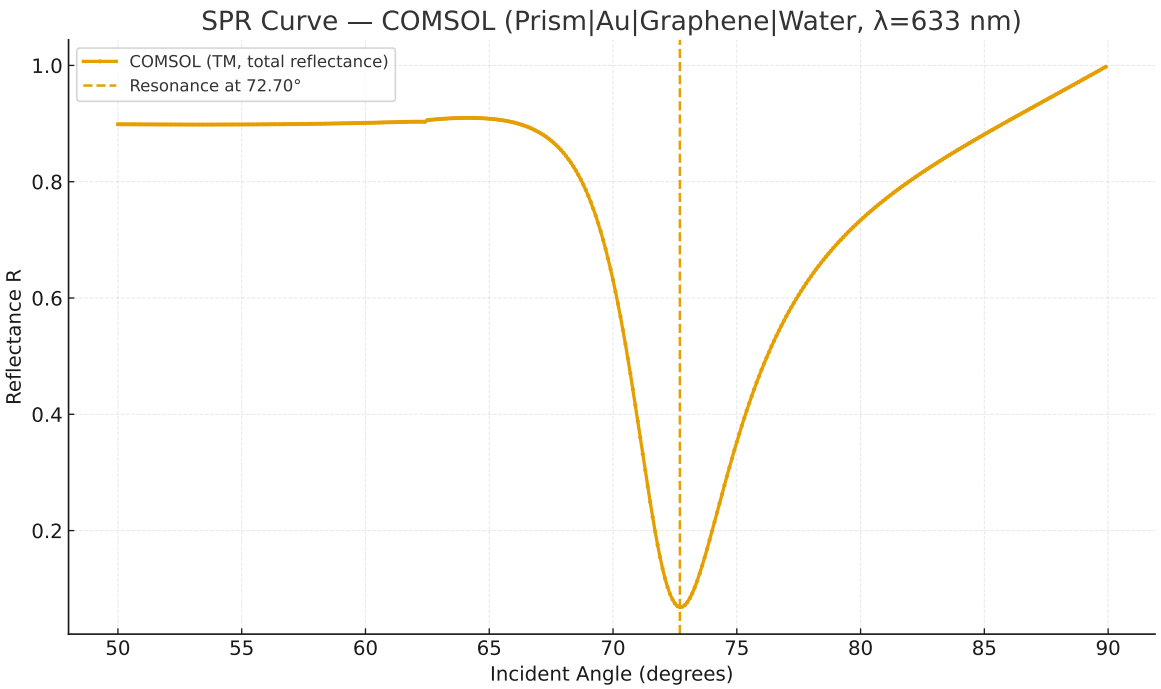

Figure 5: COMSOL TM reflectance vs. angle (Prism|Au(50 nm)|Graphene(0.34 nm)|Water, $\lambda = 633$ nm). $\theta_{\text{res}} = 72.70°$, $R_{\min} \approx 0.0684$, FWHM $\approx 5.00°$.

FEniCS setup (TM, 2D).. Scalar H_z formulation with complex ε_r; PMLs on exit/side boundaries; oblique plane-wave drive at the prism port. Graphene represented as an ultrathin film (0.34 nm, $n_g \approx 3.0 - 1.4i$), equivalent to a surface-conductivity sheet in the weak form. Strong mesh refinement across Au/graphene resolves skin depth and near fields. Angle sweep of θ provides a reflectance-like metric at the port; the dip tracks the analytical TMM trend.

COMSOL setup (Wave Optics, Frequency Domain).. Layered 2D stack with TM port at the prism side, scattering boundaries with thin PMLs on the opposite side. Au: Johnson–Christy at 633 nm; graphene: 0.34 nm thin film, $n_g \approx 3.0 - 1.4i$. Angle sweep returns $R(\theta)$ with a pronounced minimum at $\theta_{\text{res}} \approx 72.7°$, consistent with the expected Kretschmann resonance in water.

8. Conclusion

We outlined a compact workflow to model SPR in prism–Au–graphene structures at $\lambda = 633$ nm. Analytical TMM provides a reliable benchmark; FEniCS and COMSOL reproduce the resonance angle and overall line shape with small differences attributable to discretization and boundary treatments. The setup is suitable for quick sensitivity studies (e.g. Δn in water) and thickness optimization of the metal film.

References

[1] E. Kretschmann, H. Raether, Radiative decay of non-radiative surface plasmons excited by light, Zeitschrift für Naturforschung A 23 (1968) 2135.

[2] C. Project, Simulation of the surface plasmon resonance (spr) using kretschmann configuration, course Mini Project Description (2025).

[3] M. N. O. Sadiku, Elements of Electromagnetics, Oxford University Press, 2015.

[4] H. Raether, Surface Plasmons on Smooth and Rough Surfaces and on Gratings, Springer, 2014.

[5] P. B. Johnson, R. W. Christy, Optical constants of the noble metals, Physical Review B 6 (1972) 4370–4379.

[6] V. K. Dien, W.-B. Li, K.-I. Lin, N. T. Han, M.-F. Lin, Electronic and optical properties of graphene, silicene, germanene, and their semi-hydrogenated systems, RSC Advances 12 (2022) 34851–34865.

[7] B. Kacerovská, Modeling of plasmonic nanostructures in comsol, diploma Thesis, VŠB–TU Ostrava (2017).